Urban Heat Island Growth Modeling Using Artificial Neural Networks and Support Vector Regression: A case study of Tehran, Iran

SH. A. Sherafati [a], M. R. Saradjian [b], S. Niazmardi [c]

Remote sensing division, Department of surveying Engineering,
College of engineering, University of Tehran, Tehran, Iran
[a] sh.sherafati@alumni.ut.ac.ir
[b] sarajian@ut.ac.ir
[c] s.niazmardi@ut.ac.ir

KEY WORDS: Urban Heat Island, Artificial Neural Networks, Satellite Images, Land Surface Temperature

ABSTRACT:

Numerous investigations on Urban Heat Island (UHI) show that land cover change is the main factor of increasing Land Surface Temperature (LST) in urban areas. Therefore, to achieve a model which is able to simulate UHI growth, urban expansion should be concerned first. Considerable researches on urban expansion modeling have been done based on cellular automata. Accordingly the objective of this paper is to implement CA method for trend detection of Tehran UHI spatiotemporal growth based on urban sprawl parameters (such as Distance to nearest road, Digital Elevation Model (DEM), Slope and Aspect ratios). It should be mentioned that UHI growth modeling may have more complexities in comparison with urban expansion, since the amount of each pixel's temperature should be investigated instead of its state (urban and non-urban areas). The most challenging part of CA model is the definition of Transfer Rules. Here, two methods have used to find appropriate transfer Rules which are Artificial Neural Networks (ANN) and Support Vector Regression (SVR). The reason of choosing these approaches is that artificial neural networks and support vector regression have significant abilities to handle the complications of such a spatial analysis in comparison with other methods like Genetic or Swarm intelligence. In this paper, UHI change trend has discussed between 1984 and 2007. For this purpose, urban sprawl parameters in 1984 have calculated and added to the retrieved LST of this year. In order to achieve LST, Thematic Mapper (TM) and Enhanced Thematic Mapper (ETM+) night-time images have exploited. The reason of implementing night-time images is that UHI phenomenon is more obvious during night hours. After that multilayer feed-forward neural networks and support vector regression have used separately to find the relationship between this data and the retrieved LST in 2007. Since the transfer rules might not be the same in different regions, the satellite image of the city has divided to several parts and for each part a specific CA model has defined. In the training step some pixels have randomly selected to calibrate the neural network and the regression. Then, using the trained neural network and support vector regression, LST in year 2007 has retrieved for all pixels. Results have indicated a great relationship between the simulated LST and the real one which has retrieved from thermal band of satellite image in 2007 ($r = 0.843$ for ANN method and $r = 0.856$ for SVR method). Although SVR caused to a better result, this method is much more time consuming than ANN method, especially when the number of training pixels increase.

1. INTRODUCTION

Difference in temperature between urban and its surrounding rural areas creates Urban Heat Island (UHI). Advent of remote sensing technology makes it possible to study more comprehensively this phenomenon. Lots of factors affect creation of this temperature discrepancy. Chen, et al., (2005) applied artificial neural networks to carry out the correlation between LST and factors like land-cover, population density, energy consumption and water ratio in urban area (Chen, et al., 2005). However, numerous studies on urban climate have shown that the most affective factor on UHI is the land-cover change especially conversion of vegetation and bare soil to concrete, asphalt and other man-made structures (Dousset & Gourmelon, 2003) (Pu, et al., 2006). On the other hand, other human activities especially those cause to burning fossil fuels, which increase the amount of carbon dioxide, may raise temperature in global scale in comparison with small scales (urban area). Therefore, to achieve a model which is able to simulate UHI, urban expansion should be concerned first.
Considerable researches on urban expansion modeling have been done based on cellular automata (White, et al., 1997) (Gar-On Yeh & Li, 2002) (Alkheder & Shan, 2005). In CA models there is a grid of cells, each in one of a finite number of states. The goal of CA is modeling how these states of cells change in discrete time steps (Menard & Marceau, 2005). In this study, to find the CA model's transfer rules, Artifitial Neural Networks and Support Vector Regression have been implemented seperately and the ability and acuracy of these methods have been compared.

2. STUDY AREA AND DATA SET

2.1 Study Area

Tehran is located in the North of central part of Iran (52°E, 35°N) with a population over 8 million. It has semi dry and semi cold climate. The elevation difference in the northern and southern parts of the city is about 900 meter which causes significant difference in the city's temperature. Increasing of the population in the last three decades causes to converting lots of surrounding natural land-covers to the urban structures.

2.2 Data Sets

TM and ETM+ on board Landsat4 and Landsat5 have spatial resolution of 30 meters in thermal band respectively. These sensors images are capable to be classified to main land-cover types and retrieve LST. Another remotely sensed data

implemented here is SRTM[1] digital elevation model which provides other spatial information like slope and aspect ratios in addition to altitude as urban sprawl parameters.
Aside from satellite images, auxiliary data such as road layers has been used for developing transportation network.

3. METHODOLOGY

3.1 LST Retrieval

Each of the LANDSAT sensors has unique calibration coefficients. Digital numbers are converted to top-of-atmospheric TOA radiance (R_{toa}) using a linear equation (Weng, et al., 2004):

$$R_{toa} = G \times DN + b$$

G and b can be obtained from the header file of LANDSAT images. Then TOA radiance is converted to at-satellite brightness temperature with the following invers Planck's equation (Almeida, et al., 2008):

$$T = \frac{K_2}{\ln\left(\frac{K_1 \times \varepsilon}{R_{toa}} + 1\right)}$$

Where coefficients K_1 and K_2 are shown in table1.

Table 1. coefficients of inverse of Plank's equation for Landsat sensors

	Landsat TM	Landsat ETM+
K_1	607.76	666.09
K_2	1260.56	1282.71

But Difference in blackbody and land surface emissivity and also atmospheric effects make discrepancy between brightness temperature and land surface temperature. The usual method for driving land surface emissivity is using a vegetation index like NDVI. (Sobrino et al) proposed a method for retrieving emissivity from NDVI as follows (Sobrino, et al., 2004):

$$NDVI = \frac{band4 - band3}{band4 + band3}$$

$$\varepsilon = 0.004 \times \left(\frac{NDVI - 0.2}{0.5 - 0.2}\right)^2 + 0.9 \qquad 0.2 < NDVI < 0.5$$

$$\varepsilon = 0.99 \qquad NDVI > 0.5$$

$$\varepsilon = 0.97 \qquad NDVI < 0.2$$

According to the calculated emissivity, LST is retrieved from brightness temperature (Hu & Jia, 2009).

$$LST = \frac{T}{1 + (\lambda \times T/\rho)\ln \varepsilon}$$

Where λ =11.5 and ρ=1.438×10^{-2} mK.
To perform atmospheric correction in sensors like ETM+ and TM which have only one thermal band, the primary method is to use radiative transfer model like LOWTRAN, MODTRAN and WINDOW, coupled with knowledge about atmospheric structures like pressure, temperature and humidity profile (Kerr, et al., 2005). The existence of enough metrological stations that produce atmospheric information and the synchronism of this data with satellite imaging time are two major problems that can impact atmospheric correction methods using these radiative transfer codes. But in local studies like UHI monitoring there are some alternatives to do atmospheric correction. Xu, et al., (2009) apply a normalization technique and rescaling LST between 0 and 1 as follows:

$$LST' = \frac{(LST_i - LST_{min})}{(LST_{max} - LST_{min})}$$

Where LST' is the normalized forLST, LST_i is the LST value for pixel i, and LST_{min} and LST_{max} are the minimum and maximum LST values of the LST image (Xu, et al., 2009).
Another approach is to use Difference Land Surface Temperature (ΔLST) instead of LST which can achieve as follows:

$$\Delta LST = LST_i - LST_{base}$$

Where LST_{base} is the mean temperature of a selected area in southwest of Tehran in which landcover types have not changed during last decades. The advantage of using ΔLST or LST' instead of LST_p is that some sources of systematic errors like radiometric calibration errors and atmospheric effects are partially removed in the differencing or normalization procedure (Fabrizi, et al., 2010) (Xu, et al., 2009).

3.2 Neural Networks for UHI Modelling

UHI growth may have more complexities in comparison with urban expansion (since the amount of each pixel's temperature should be investigated instead of its state). Artificial intelligence and especially neural networks have significant abilities to handle the complications of such a spatial analysis (Gar-On Yeh & Li, 2002). Although neural network has more flexibilities to solve this simulation (in comparison with other artificial intelligence methods like Genetic or Swarm intelligence), as a black box it has some disadvantages. As an illustration, the main problem is that neural network does not determine the role of each site attribute in land-cover change.
Here, the multilayer perceptron (MLP) neural network has been used to model how UHI has changed between 1984 and 2007 considering urban expansion. Therefore, defining suitable site attributes is crucial in proposed method. In this study, five spatial variables have been defined as urban sprawl parameters, which include:

1. **Neighborhood development level** which determines the number of urban pixels in a predefined neighborhood size. This parameter can derive from classified images. The Satellite image has been classified to the classes of urban area, bare soil and vegetation using maximum likelihood algorithm. Defining the size of the neighborhood is based on image spatial resolution and the difference between simulation time steps.
2. **Distance to nearest road** as an important urban sprawl parameter that can greatly determine the direction of urban expansion.
3. **Digital Elevation Model (DEM).** This parameter affects both urban expansion directions and LST
4. **Slope** which is derived from DEM and has influence on urban expansion and LST. Zhao, et al., (2007) discussed the relationship of north and south slope on LST.

[1] Shuttle Radar Topography Mission

5. **Aspect.** This parameter which is also derived from DEM has unique effect on LST especially in rough areas because of the sun shadow.

It should be noted that in urban expansion studies, it is not essential to use all the parameters of slope, aspect and elevation together, but as each of them has its unique impacts on temperature, we consider all of them here. Figure 1 shows the structure of proposed neural network for UHI simulation.

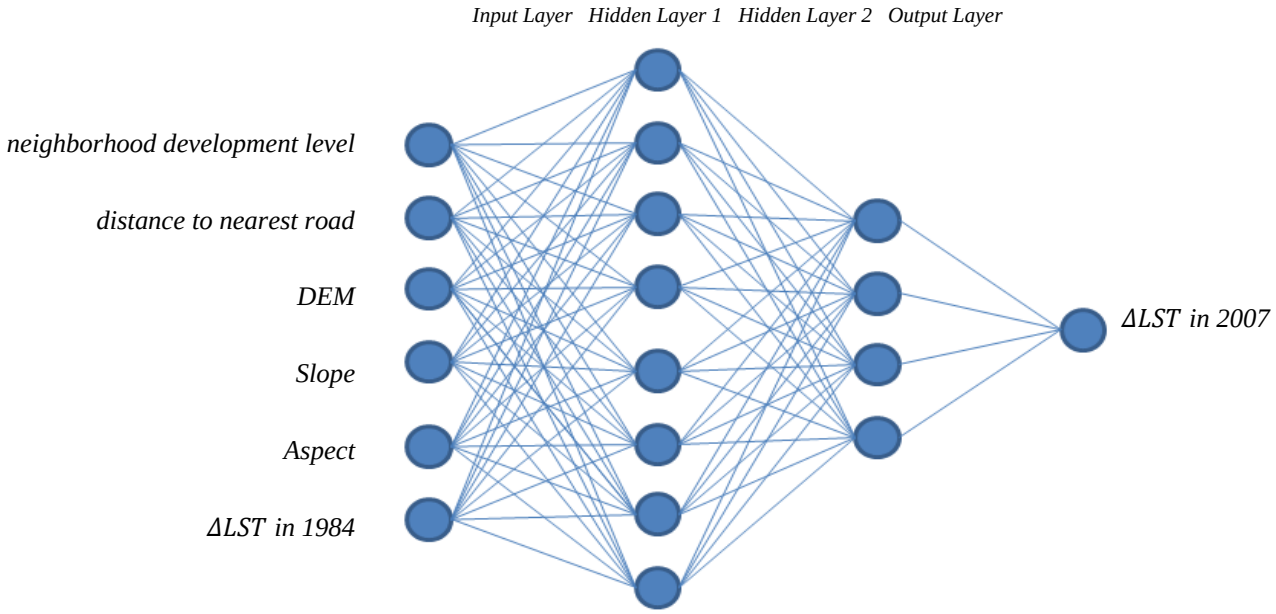

Figure 1. Configuration of proposed ANN for simulation of UHI

In the training phase, a number of random pixels have been chosen. Site attributes for the selected pixels have been calculated and given to the neural network as its inputs. All site attributes have been scaled into the range of [0, 1] to make sure that all parameters are equally affective in neural network model (Sobrino, et al., 2004). The output of neural network, in the training step, is LST in year 2007 for the selected pixels, which have been obtained from Landsat7 ETM+ night-time image. Therefore the neural network has six neurons in its input layer and one neuron as output layer. There is no specific way to determine number of hidden layers and their neurons. However, there are some suggestions that can help to design neural network hidden layers. For instance in Kolmogorov's theorem a continuous function $Ø: X^n \rightarrow R^c$ can be represented by a neural network with n neurons in its input layer, (2n+1) neurons in its single hidden layer and c neurons which forms the output layer (Almeida, et al., 2008). Gar-On Yeh, et al., (2002) indicated that a network with (2n/3) neurons in one hidden layer can generate results of almost the same accuracy level, compared with (2n+1) neurons in the hidden layer but consumes much less time for training (Gar-On Yeh & Li, 2002). In this paper multiple neural networks with different number of hidden layers and neurons were tested. There wasn't significant difference between them. The proposed neural network has two hidden layers with eight and four neurons in its first and second ones respectively. It should be noted that large number of hidden layers and neurons can extremely increase the training time.

3.3 Support Vector Regression for UHI Modelling

Support Vector Regression (SVR) is a new supervised learning method which emerged in late 1970s (Vapnik, 1979). SVR allows computing a powerful nonparametric approximation of the relationship between site attributes and UHI change. This technique is also used in many remote sensing applications like LST and SST retrieval (Moser, et al., 2009), leaf area index estimation and other biophysical parameter estimation from multispectral satellite images (Durbha, et al., 2007).

The most advantage of SVR, in comparison with ANN, is its ability to find global optimized result instead of local optimized one (Tso & Mather, 2009). Here we use Gaussian radial basis function as the SVR Kernel:

$$f_{(x)} = \sum_{i=1}^{n} \alpha_i \langle Q(x_i), Q(x) \rangle + b$$

$$\langle Q(x_i), Q(x) \rangle = exp\left(-\|x_i - x_j\|^2\right) \quad \gamma > 0$$

4. IMPLEMENTATION

Satellite images can explicitly display how Tehran has been expanded since 1984. Figure 2a and 2b shows the color combination of bands 4, 3 and 2 of Landsat TM and ETM+ in 1984 and 2007. Clear influence of this expansion on UHI has shown in figure 3c and 3d which were derived from thermal bands of TM and ETM+ nighttime images. The correlation between these two LST images is about 0.73

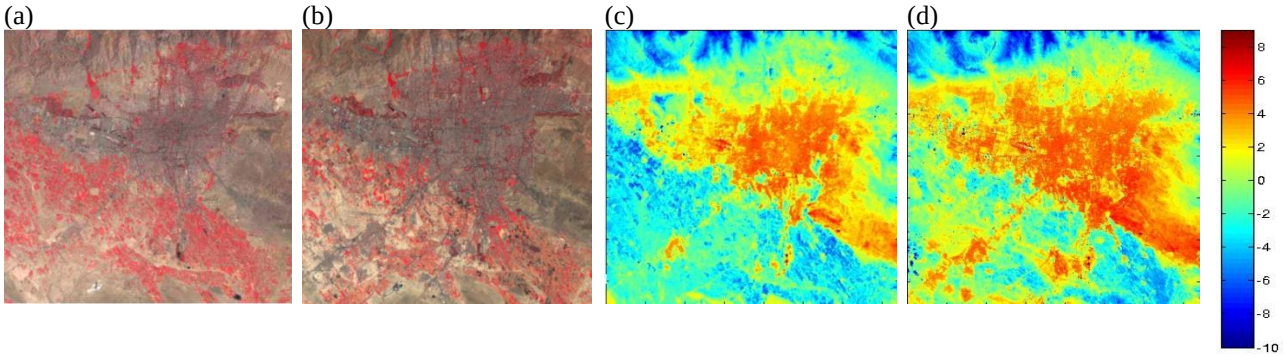

Figure 2. (a) False color combination of Landsat bands (4-3-2) in TM 1984, (b) ETM+ 2007, ΔLST derived from nighttime Landsat images in (c) 1984 and (d) 2007.

Comparing visible and thermal images in figure 2 clearly indicates the influence of land-cover types on UHI. Vegetation regions (which appear red in 4-3-2 color combination) are cooler than bare soil and urban areas. Cold mountainous areas in north of Tehran, show the effect of altitude in decreasing the LST.

After training step, the fixed neural network and trained support vector regression, are able to simulate UHI. To do this, site attributes for all of the pixels have been given to them and the simulated UHI in 2007 has been computed. Figure 3a and 3b shows LST derived from ETM+ in 2007 and the simulated UHI for this year achieved by ANN method.

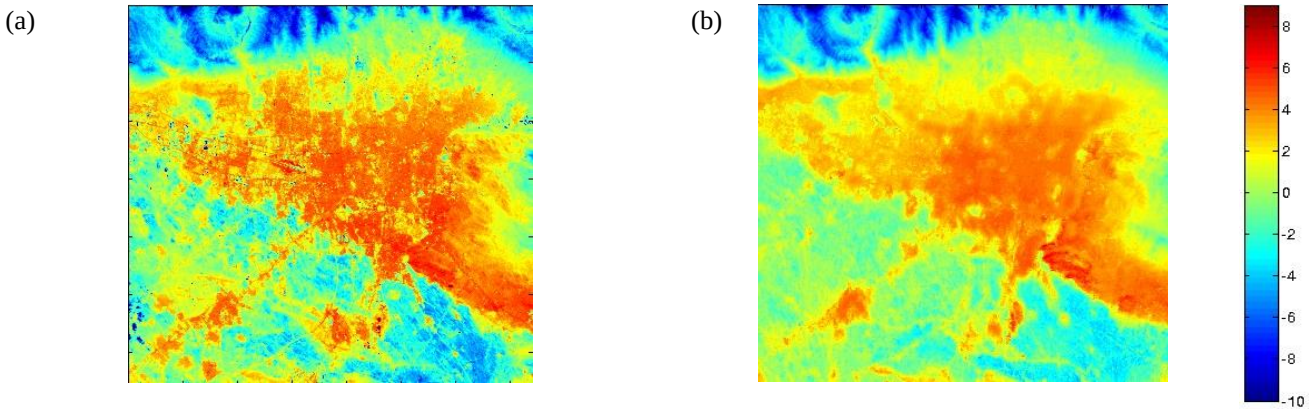

Figure 3. (a) ΔLST in 2007 derived from ETM+ nighttime image, and (b) simulated ΔLST computed from proposed model

Table2 indicates the affection of number of training pixels on result's accuracy. It is concluded that with less number of training pixels, SVR can find the transfer rules much better than ANN but by increasing the number of training pixels, both methods have almost same correlation coefficients.

Table2, relationship of training data numbers and accuracy of the results

Training data number (pixels)	50	100	500	1000	2000	5000
Correlation coefficient between real and ANN simulated ΔLST	0.55	0.72	0.78	0.82	0.82	0.84
Correlation coefficient between real and SVR simulated ΔLST	0.77	0.80	0.82	0.83	0.84	0.85

For discussing the role of neighborhood development level in the simulation model, seven windows with different size have been tested. Table3 shows the influence of size of neighborhood windows in computed correlation of real and simulatedΔLST.

Table 3. relationship between neighborhood size and computed correlation

Neighborhood Radius	1 cell	2 cell	5 cell	10 cell	20 cell	30 cell	40 cell
Correlation coefficient between real and simulated ΔLST	0.834	0.839	0.840	0.843	0.844	0.840	0.840

Table 1 indicates that the best radius for computing neighborhood is 20 pixels. However, as it was mentioned before, the proper neighborhood size depends on data spatial resolution and difference between simulation time steps.

Using the trained neural network it is feasible to simulate UHI at next time step (2030). In this case, neighborhood development level and distance to nearest road should be recomputed for year 2007, and ΔLST of input layer should be derived from ETM+ 2007 thermal band. Other site attributes in input layer are invariant.

5. CONCLUSION

Satellite thermal images have been used for simulation of Tehran UHI growth. As land-cover types extremely affect UHI, the developed simulation model is based on urban expansion. Artificial neural networks and support vector regression were used separately to find the relationship between LST in 1984 and 2007 by considering urban sprawl parameters. Great compatibility of ANN and SVR techniques, cause to strong correlation between real and simulated LSTs ($r \approx 0.844$ for ANN and $r \approx 0.856$ for SVR). However, as a disadvantage of neural networks and support vector regression, proposed models couldn't explicitly define the role of each site attribute on UHI growth. Simulation with different number of training pixels indicated that when less training pixels are used, SVR has a better estimation than ANN. This is because SVR method is more capable in finding the global optimized results.

Additionally, different sizes of windows have been implemented for determination of neighborhood development level. The best result was achieved for the 41×41 pixel size window (20 radius neighborhood).

REFERENCES

Alkheder, S. & Shan, J., 2005. *Cellular Automata Urban Growth Simulation and Evaluation- A Case Study of Indianapolis.* Ann Arbor, Michigan, USA, University of Michigan, s.n.

Almeida, C. M., Gleriani, J. M., Castejon, E. F. & Soares-Filho, B. S., 2008. Using neural networks and cellular automata for modelling intra-urban land-use dynamics. *International Journal of Geographical Information Science,* 9(22), pp. 943-963.

Chen, Y., Li, X. & Fan, Y., 2005. *Analysis of Urban Heat Island Using a Remote Sensing Model.* s.l., s.n.

Dousset, B. & Gourmelon, F., 2003. Satellite multi-sensor data analysis of urban surface temperatures and landcover. *PHOTOGRAMMETRY & REMOTE SENSING,* pp. 43-54.

Durbha, S., King, R. L. & Younan, N. H., 2007. Support vector machines regression for retrieval of leaf area index from multiangle imaging spectroradiometer. *Remote Sens. Environ,* Volume 107, pp. 348-361.

Fabrizi, R., Bonafoni, S. & Biondi, R., 2010. Satellite and Ground-Based Sensor for the Urban Heat Island Analysis in the City of Rome. *Remote Sensing,* pp. 1400-1415.

Gar-On Yeh, A. & Li, X., 2002. *Urban Simulation Using Neural Networks and Cellular Automata for Land Use Planning.* Ottawa, s.n.

Gar-On Yeh, A. & Li, X., 2002. *Urban Simulation Using Neural Networks and Cellular Automata for Land Use Planning.* Ottawa, ISPRS .

Hu, Y. & Jia, G., 2009. Influence of land use change on urban heat island derived from multi-sensor data. *INTERNATIONAL JOURNAL OF CLIMATOLOGY,* 9(30), pp. 1382-1395.

Kerr, Y. H., Lagouarde, J. P., Nerry, F. & Ottle, C., 2005. Land surface temperature retrieval techniques and applications. In: *Thermal Remmote Sensing in Land Surface Processes.* Boca Raton London New York Washington, D.C.: CRC PRESS, pp. 33-109.

Menard, A. & Marceau, D. J., 2005. Exploration of spatial scale sensitivity in geographic cellular automata. *Environment and Planning B: Planning and Design,* Volume 32, pp. 693-714.

Moser, G., Serpico & B, S., 2009. Automatic Parameter Optimization for Support Vector Regression for Land and Sea Surface Temperature Estimation From Remote Sensing Data. *Temperature Estimation From Remote Sensing Data,* 3(47), pp. 909-921.

Pu, R., Gong, P., Michishita, R. & Sasagawa, T., 2006. Assesment of multi-resolution and multi-sensor data for urban surface temperature retrieval. *Remote Sensing of Environment,* pp. 211-225.

Sobrino, J. A., Jimenez-Munoz, J. C. & Polini, L., 2004. Land surface temperature retrieval from LANDSAT TM5. *Remote Sensing of Environment,* pp. 434-440.

Sobrino, J. A., Jimenez-Munoz, J. C. & Polini, L., 2004. Land surface temperature retrieval from LANDSAT TM5. *Remote Sensing of Environment,* pp. 434-440.

Tso, B. & Mather, P. M., 2009. *CLASSIFICATION METHODS FOR REMOTELY SENSED DATA.* 2nd ed. s.l.:Taylor & Francis Group, LLC.

Vapnik, V., 1979. *Estimation of dependences based on empirical data.* Nauka, Moscow, Springer-Verlag.

Weng, Q., Lu, D. & Schubring, J., 2004. Estimation of land surface temperature-vegetation abundance ralationship for urban heat island studies. *Remote Sensing of Environment,* pp. 467-483.

White, R., Engelen, G. & Uijee, I., 1997. The use of constrained cellular automata for high-resolution modelling of urban land-use dynamics. *Environment and planning,* III(24), pp. 323-343.

Xu, H., Ding, F. & Wen, X., 2009. Urban Expansion and Heat Island Dynamics in the Quanzhou Region, China. *Selected Topics in Applied Earth Observations and remote Sensing, IEEE Journal,* 2(2), pp. 74-79.

Zhao, D., Zhang, W. & Yong, B., 2007. *Analysis of thermal environment and urban heat island using remotely sensed imageryover the north and south slope of the Qinling Mountain, China.* s.l., IEEE.